

## LC-MS, GC-MS and NMR Spectroscopic Evaluation of Consciousness Energy Healing Treated Cholecalciferol (Vitamin D<sub>3</sub>)

Mahendra Kumar Trivedi<sup>1</sup> and Snehasis Jana<sup>2\*</sup>

<sup>1</sup>Trivedi Global, Inc., Henderson, USA

<sup>2\*</sup>Trivedi Science Research Laboratory Pvt. Ltd., Thane (W), India.

Received June 05, 2019; Accepted June 12, 2019; Published September 24, 2019

### ABSTRACT

Cholecalciferol (vitamin D<sub>3</sub>) is a fat-soluble vitamin, which is widely used for the prevention and treatment of vitamin D deficiency. The aim of the study was to investigate the impact of the Trivedi Effect<sup>®</sup>-Consciousness Energy Healing Treatment on the isotopic abundance ratios ( $P_{M+1}/P_M$  and  $P_{M+2}/P_M$ ) along with the structural properties of vitamin D<sub>3</sub> using advanced spectroscopy methods. Vitamin D<sub>3</sub> sample was divided into two parts, one part of the sample was termed as a control sample, while the other part of the sample received the Trivedi Effect<sup>®</sup> (Biofield Energy Treatment) remotely by a famous Biofield Energy Healer, Mr. Mahendra Kumar Trivedi termed as the Biofield Energy Treated sample. The liquid chromatography-mass spectrometry (LC-MS) chromatograms of both the cholecalciferol samples showed a single largest peak at the retention time ( $R_t$ ) 20.6 min and protonated molecular mass peak at  $m/z$  385.3 (calcd for  $C_{27}H_{45}O^+$ , 385.35) in the mass spectra. The LC-MS based isotopic abundance ratios of  $P_{M+1}/P_M$  ( $^2H/^1H$  or  $^{13}C/^12C$  or  $^{17}O/^16O$ ) and  $P_{M+2}/P_M$  ( $^{18}O/^16O$ ) were significantly increased by 15.20% and 10.44%, respectively in the treated cholecalciferol compared to the control sample. Thus, the  $^{13}C$ ,  $^2H$  and  $^{17}O$  contributions from  $C_{27}H_{45}O^+$  to  $m/z$  386 and  $^{18}O$  contribution from  $C_{21}H_{21}O_6^+$  to  $m/z$  387 in the treated sample was significantly increased compared with the control sample. The gas chromatography-mass spectrometry (GC-MS) spectral data showed that the molecular mass peak intensities ( $m/z$  384.4) in the treated cholecalciferol at  $R_t$  23.28 and 23.88 min were increased by 4.54% and 3.21%, respectively compared with the control sample. The proton and carbon signals for  $CH_3$ ,  $CH_2$ ,  $CH$ ,  $C-OH$  and  $=C=$  groups in the  $^1H$  and  $^{13}C$  Nuclear Magnetic Resonance (NMR) spectra of the treated and control samples were similar. The improvement in the isotopic abundance ratios and mass peak intensities of the treated cholecalciferol might be due to the possible mediation of neutrinos via the Trivedi Effect<sup>®</sup>-Consciousness Energy Healing Treatment. The increased isotopic abundance ratio of the treated cholecalciferol might have a stronger atomic bond, increase the stability and alter the rate of metabolic reactions in the body. Thus, the Biofield Energy Treated cholecalciferol would be more efficacious nutraceutical and pharmaceutical formulations which might provide better therapeutic response counter to deficiency of vitamin D, rickets, osteoporosis, diabetes mellitus, cancer, cardiovascular diseases, infections, etc.

**Keywords:** Cholecalciferol, The Trivedi Effect<sup>®</sup>, Energy of consciousness healing treatment, LC-MS, Isotopic abundance, GC-MS, Kinetic isotope effects

### INTRODUCTION

Cholecalciferol (vitamin D<sub>3</sub>) is found in foods and also in the dietary supplement to overcome vitamin deficiency and associated disease [1]. It has multiple effects on the human body, which regulate the functions of muscles, brain, lungs, liver, kidneys, heart, immune system, pancreas, large and small intestines. Vitamin D receptors are ubiquitously found in most of the body parts. Vitamin D receptor response elements with hundreds of genes directly or indirectly influence cell-to-cell communication, normal cell growth, cell cycling and proliferation, cell differentiation, maintenance of calcium and phosphorus balance, hormonal

balance, neurotransmission, skin health, immune and cardiovascular functions [1-3]. Deficiency of vitamin D occurs in those who have an insufficient dietary intake or

**Corresponding author:** Snehasis Jana, Trivedi Science Research Laboratory Pvt. Ltd., Thane (W), Maharashtra, India, Tel: +91-022-25811234; E-mail: publication@trivedieffect.com

**Citation:** Trivedi MK & Jana S. (2019) LC-MS, GC-MS and NMR Spectroscopic Evaluation of Consciousness Energy Healing Treated Cholecalciferol (Vitamin D<sub>3</sub>). J Chem Sci Eng, 2(3): 110-121.

**Copyright:** ©2019 Trivedi MK & Jana S. This is an open-access article distributed under the terms of the Creative Commons Attribution License, which permits unrestricted use, distribution, and reproduction in any medium, provided the original author and source are credited.

who fail to produce enough vitamin D<sub>3</sub> in their skin from its precursor, 7-dehydrocholesterol, in response to exposure to ultraviolet light. Vitamin D deficiency conditions also caused by intestinal malabsorption or chronic liver disease, familial hypophosphatemia, and for the hypocalcaemia that is associated with hypoparathyroidism [2]. Vitamin D shortage in the body plays a critical role in several diseases, e.g. rickets, osteoporosis, arthritis, multiple sclerosis, cancer, diabetes mellitus, mental disorders, cardiovascular diseases, infections, cognitive impairment in older adults, Parkinson's and Alzheimer's diseases, dementia, glucose intolerance, multiple sclerosis, etc. [3-6]. In the USA, 15 µg/d (600 IU per day) is required for all individuals between all the age group [7]. High dose vitamin D supplementation may cause toxicity like hypercalcemia, polyuria, polydipsia, weakness, mental retardation and insomnia [8]. Vitamin D stability is more concerned as it is a heat and light-sensitive compound [9,10]. The transformation mechanism of vitamin D and the absorption of its active form (vitamin D<sub>3</sub>) are very complicated. Vitamin D<sub>3</sub> bioavailability directly affected by various factors such as dietary fiber, genetic factors and the status of vitamin D<sub>3</sub> [11].

Recent studies revealed that the bioavailability profile of several pharmaceutical/nutraceutical compounds, i.e., 25-hydroxyvitamin D<sub>3</sub> [25(OH)D<sub>3</sub>], resveratrol, berberine, etc. are significantly altered by means of the Trivedi Effect<sup>®</sup>-Consciousness Energy Healing Treatment [12-14]. The "Biofield Energy" is a type of electromagnetic energy field generated by continuous moment of the charged particles (i.e., cells, ions, etc.) in the human body [15,16]. The Biofield Energy Healers has the ability to harness the energy from the "Universal Energy Field" and can transfer into any object(s) around the globe. The process of treatment to an object is known as the Biofield Energy Healing Treatment. There are several Energy Therapies that are used nowadays against various disease conditions [17,18]. The Energy Therapy has been recognized worldwide as a Complementary and Alternative Medicine health care approach by the National Center of Complementary and Integrative Health with other therapies, medicines and practices such as Qi Gong, Tai Chi, Ayurvedic medicine, traditional Chinese herbs and medicines, aromatherapy, meditation, yoga, chiropractic/osteopathic manipulation, acupressure, homeopathy, acupuncture, healing touch, hypnotherapy, movement therapy, Reiki, cranial sacral therapy, etc. [19]. The Trivedi Effect<sup>®</sup> has surprising ability to transform the characteristic properties of metals and ceramic [20, 21], organic compounds [22,23], nutraceuticals [24], pharmaceuticals [25,26], culture medium [27,28] and improve the overall productivity of crops [29], alteration of the isotopic abundance ratio in the organic compounds [30-32] may be through the possible mediation of neutrinos [15].

There are wide applications of study on the natural stable isotope ratio analysis in several fields of sciences to understand the isotope effects resulting from the alterations

of the isotopic composition [33-35]. Gas chromatography-mass spectrometry (GC-MS) and liquid chromatography-mass spectrometry (LC-MS), are widely used for the analysis of isotope ratio with sufficient precision [34]. Thus, the isotopic abundance ratio analysis of P<sub>M+1</sub>/P<sub>M</sub> (<sup>2</sup>H/<sup>1</sup>H or <sup>13</sup>C/<sup>12</sup>C or <sup>17</sup>O/<sup>16</sup>O) and P<sub>M+2</sub>/P<sub>M</sub> (<sup>18</sup>O/<sup>16</sup>O) was performed to evaluate the influence of the Trivedi Effect<sup>®</sup> on the isotopic abundance ratio in cholecalciferol. Similarly, the LC-MS, GC-MS and NMR (Nuclear Magnetic Resonance) techniques were also used to characterize the structural properties of cholecalciferol.

## MATERIALS AND METHODS

### Chemicals and reagents

The test sample cholecalciferol (>98%) was purchased from Sigma-Aldrich, India but other chemicals used during the experiments were of analytical grade purchased in India.

### Consciousness energy healing treatment strategies

The test sample cholecalciferol was divided into two equal parts. One part of the test cholecalciferol was considered as a control sample, which was not received the Biofield Energy Treatment. Whereas, the second part was received the Consciousness Energy Healing Treatment (Trivedi Effect<sup>®</sup> for 3 min) remotely under standard laboratory conditions and known as treated cholecalciferol. This Biofield Energy was provided through the healer's unique energy transmission process by a famous Biofield Energy Healer, Mr. Mahendra Kumar Trivedi (USA), to the test item. The control cholecalciferol was treated with a "sham" healer, who did not have any knowledge about the Biofield Energy Treatment. After the treatment both the samples of cholecalciferol were kept in sealed conditions and characterized.

### Characterization

**Liquid chromatography-mass spectrometry (LC-MS) analysis and calculation of isotopic abundance ratio:** The LC-MS analysis of the samples was carried out with the help of LC-Dionex Ultimate 3000, MS-TSQ Endura, USA equipped with a photo-diode array (PDA) detector connected with a triple-stage quadrupole mass spectrometer (Thermo Scientific TSQ Endura, USA) with a Thermo Scientific Ion Max NG source and Atmospheric Pressure chemical ionization (APCI). The analysis was performed on a reversed phase Zorbax SB-C18 100 × 4.6 mm, 3.5 µm in gradient mode in the liquid chromatograph (column temperature 40°C). The mobile phase was ammonium formate and 0.5% formic acid in water (A) and acetonitrile (B) at a constant flow rate of 0.6 mL/min. The injection volume was 10 µL and the total run time was 30 min. Chromatographic separation was achieved using gradient condition as follow: 0 min-50% B, 5 min-90% B, 10 min-100% B, 20 min-100% B, 25 min-50% B and 30 min-50%

B. Peaks were monitored using the PDA detector. The mass spectrometric analysis was performed under +ve ESI mode.

The natural abundance of C, O and H isotope can be predicted from the comparison of the relative abundance of the isotope peak with respect to the base peak. The values of the natural isotopic abundance of the common elements are obtained from the literature [36-39]. The change in the isotopic abundance ratios ( $P_{M+1}/P_M$  and  $P_{M+2}/P_M$ ) for the control and treated cholecalciferol was calculated using equation (1).

$$\% \text{ Change in isotopic abundance ratio} = \left[ \frac{IAR_{\text{Treated}} - IAR_{\text{Control}}}{IAR_{\text{Control}}} \times 100 \right] \quad (1)$$

Where  $IAR_{\text{Treated}}$  and  $IAR_{\text{Control}}$  is the isotopic abundance ratio in the treated and control cholecalciferol, respectively.

#### Gas chromatography-mass spectrometry (GC-MS)

**analysis:** An Agilent 7890B GC equipped with a silica capillary column HP-5 MS (30 m × 0.25 mm × 0.25 μm) and coupled to a quadrupole detector with pre-filter (5977B, USA) was operated with electron impact (EI) ionization in positive mode at 70 eV. The oven temperature was programmed from 50°C (1 min hold) to 150°C @ 20°C/min to 200°C (6 min hold) @ 25°C/min to 280°C @ 20°C/min (12 min hold). Temperatures of the injector, detector (FID), auxiliary, ion source and quadrupole detector were 230, 250, 280, 230 and 150°C. Cholecalciferol was dissolved in methanol, and 5.0 μL was splitlessly injected with helium as a carrier gas with a flow rate of 2.0 mL/min.

The percent change in peak intensity (I) was calculated using the following equation (2):

$$\% \text{ Change in peak intensity (I)} = \frac{I_{\text{Treated}} - I_{\text{Control}}}{I_{\text{Control}}} \times 100 \quad (2)$$

Where,  $I_{\text{Control}}$  and  $I_{\text{Treated}}$  are the peak intensity of the control and Biofield Energy Treated sample, respectively.

**Nuclear magnetic resonance (NMR) analysis:**  $^1\text{H}$  NMR spectra of cholecalciferol were recorded at 400 MHz on Agilent-MRDD2 FT-NMR. Approximately 3 mg of the sample was dissolved in DMSO- $d_6$ . Chemical shifts (δ) were in parts per million (ppm) relative to the solvent's residual proton chemical shift  $\{(\text{CD}_3)_2\text{SO}, \delta=2.5\}$ . Similarly,  $^{13}\text{C}$  NMR spectra of cholecalciferol were measured at 100 MHz on Agilent-MRDD2 FT-NMR spectrometer at room temperature. The sample was dissolved in DMSO- $d_6$ . The solvent's residual carbon chemical shift  $\{(\text{CD}_3)_2\text{SO}, \delta=39.52\}$ .

## RESULTS AND DISCUSSION

### Liquid chromatography-mass spectrometry (LC-MS) analysis and isotopic abundance ratio analysis

The control and treated cholecalciferol showed a sharp chromatographic peak at the retention times ( $R_t$ ) of 20.63 and 20.62 min, respectively (**Figure 1**). The % peak area at  $R_t$  20.6 min was 99.58 and 99.54 in control and Biofield Energy Treated sample, respectively. This indicated that the polarity of the Biofield Energy Treated sample remained similar compared to the control cholecalciferol.

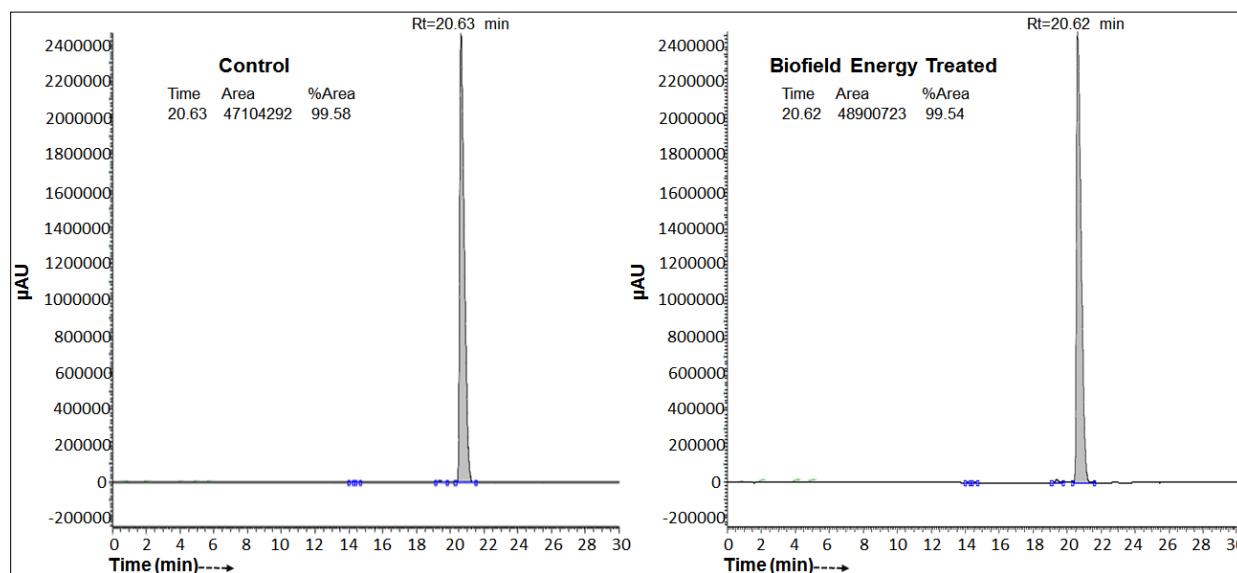


**Figure 1.** Total ion chromatograms of the control and treated cholecalciferol.

The mass spectra of the control and treated samples at  $R_t$  of 20.6 min exhibited the presence of the molecular ion of cholecalciferol ( $\text{C}_{27}\text{H}_{45}\text{O}^+$ ) adduct with hydrogen ion (**Figure 2**) at  $m/z$  385.3 (calcd for  $\text{C}_{27}\text{H}_{45}\text{O}^+$ , 385.35). The

lower  $m/z$  showed the presence of the  $[\text{M}-\text{OH}]^+$  ion mass peak at  $m/z$  367.3 (calcd for  $\text{C}_{27}\text{H}_{43}^+$ , 367.3) in both the cholecalciferol samples (**Figure 2**).

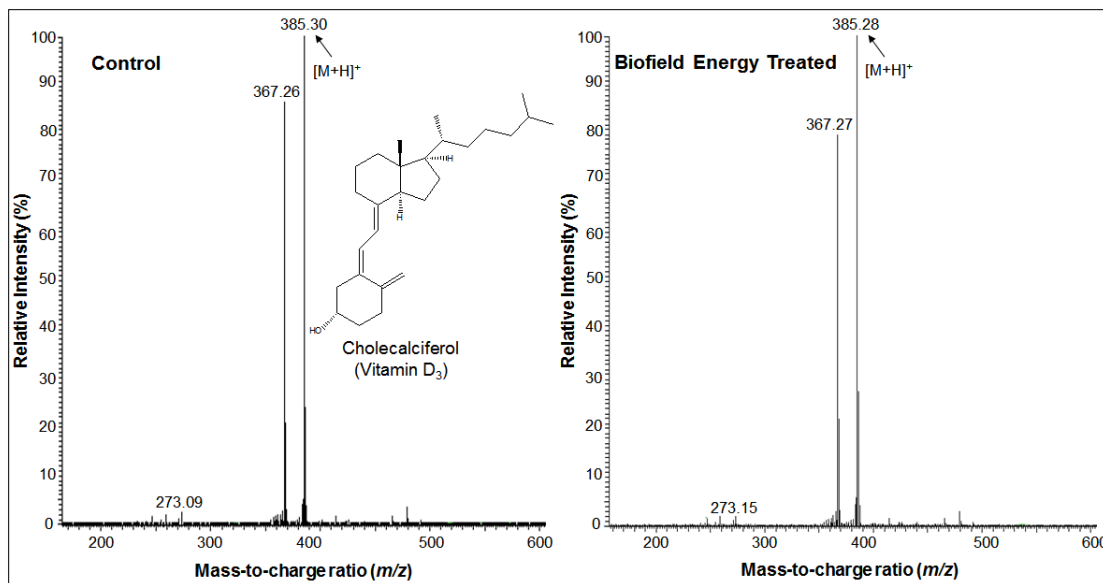


**Figure 2.** The mass spectra of the control and treated cholecalciferol at  $R_t$  20.6 min in the chromatograms.

The mass spectrum of the Biofield Energy Treated cholecalciferol showed an almost similar type of mass fragmentation pattern of the control sample (**Figure 2**). The molecular ion peak at  $m/z$  385.3 exhibited 100% relative peak intensity in both the mass spectra (**Figure 2**). The relative peak intensities of the other ion peaks in the Consciousness Energy Healing Treated cholecalciferol were significantly altered compared to the control sample.

The control and treated samples of cholecalciferol showed the mass of a protonated molecular ion at  $m/z$  385.3 (calcd for  $C_{27}H_{45}O^+$ , 385.35) with 100% relative abundance in the mass spectra. The theoretical calculation of isotopic peak  $P_{M+1}$  for the protonated cholecalciferol presented as below:

$$P(^{13}C) = [(27 \times 1.1\%) \times 100\% \text{ (the actual size of the } M^+ \text{ peak)}] / 100\% = 29.7\%$$

$$P(^2H) = [(45 \times 0.015\%) \times 100\%] / 100\% = 0.675\%$$

$$P(^{17}O) = [(1 \times 0.04\%) \times 100\%] / 100\% = 0.04\%$$

$$P_{M+1}, \text{ i.e., } ^{13}C, ^2H \text{ and } ^{17}O \text{ contributions from } C_{27}H_{45}O^+ \text{ to } m/z \text{ 386} = 30.42\%$$

Similarly, the theoretical calculation of isotopic peak  $P_{M+2}$  for the protonated cholecalciferol presented as below:

$$P(^{18}O) = [(1 \times 0.20\%) \times 100\%] / 100\% = 0.2\%$$

$$P_{M+2} \text{ of } ^{18}O \text{ contribution from } C_{27}H_{45}O^+ \text{ to } m/z \text{ 387} = 0.2\%$$

The calculated isotopic abundance of  $P_{M+1}$  value 30.42% was higher to the observed value (23.69%), but the

calculated  $P_{M+2}$  value 0.2% was lower to the observed value (3.64%) (**Table 1**). The probability of  $A+1$  and  $A+2$  elements having an isotope with one and two mass unit heavier, respectively than the most abundant isotope (i.e.,  $^{13}C$ ,  $^2H$ ,  $^{17}O$  and  $^{18}O$ ) contributions to the mass of the isotopic molecular ion  $[M+1]^+$  and  $[M+2]^+$ .  $^2H$  did not contribute much any isotopic  $m/z$  ratios because of its less natural abundance compared to the natural abundances of C and O isotopes [37,38]. From the calculations, it was observed that  $^{13}C$ ,  $^{17}O$  and  $^{18}O$  have the major contributions from cholecalciferol to the isotopic mass peak at  $m/z$  386 and 387. Therefore,  $P_M$ ,  $P_{M+1}$  and  $P_{M+2}$  of the cholecalciferol at  $m/z$  385, 386 and 387 of the control and Biofield Energy Treated samples were obtained from the experimental relative abundance of  $M^+$ ,  $(M+1)^+$  and  $(M+2)^+$  peaks, respectively in the mass spectra (**Table 1**).

The isotopic abundance ratio of  $P_{M+1}/P_M$  ( $^2H/^1H$  or  $^{13}C/^{12}C$  or  $^{17}O/^{16}O$ ) in the Trivedi Effect<sup>®</sup>-Consciousness Energy Healing Treated cholecalciferol was significantly increased by 15.20% compared to the control sample (**Table 1**). Thus, the  $^{13}C$ ,  $^2H$  and  $^{17}O$  contributions from  $C_{27}H_{45}O^+$  to  $m/z$  386 in the Biofield Energy Treated sample was significantly increased compared to the control sample. Similarly, the isotopic abundance ratio of  $P_{M+2}/P_M$  ( $^{18}O/^{16}O$ ) in the Biofield Energy Treated cholecalciferol was significantly increased by 10.44% compared to the control sample (**Table 1**). Thus, the  $^{18}O$  contribution from  $C_{27}H_{45}O^+$  to  $m/z$  387 in the Biofield Energy Treated cholecalciferol was also significantly increased compared to the control sample.



**Table 1.** LC-ESI-MS isotopic abundance ratio analysis of control and treated vitamin D<sub>3</sub>.

Parameters	Control sample	Biofield Energy Treated sample
$P_M$ at $m/z$ 385 (%)	100	100
$P_{M+1}$ at $m/z$ 386 (%)	23.69	27.29
$P_{M+1}/P_M$	0.2369	0.2729
% Change of isotopic abundance ratio ( $P_{M+1}/P_M$ ) compared to the control cholecalciferol		15.20
$P_{M+2}$ at $m/z$ 387 (%)	3.64	4.02
$P_{M+2}/P_M$	0.0364	0.0402
% Change of isotopic abundance ratio ( $P_{M+2}/P_M$ ) compared to the control cholecalciferol		10.44

$P_M$ =the relative peak intensity of the parent molecular ion  $M^+$ ;  $P_{M+1}$ =the relative peak intensity of the isotopic molecular ion  $[M+1]^+$ ,  $P_{M+2}$ =the relative peak intensity of the isotopic molecular ion  $[M+2]^+$  and  $M$ =mass of the parent cholecalciferol molecule

Neutrons and alteration in its number in the molecule lead to the increased or decreased isotopic abundance of the compounds. The changes in atomic/molecular weights are postulated to the changes in atomic mass and charge *via* the possible mediation of neutrinos [15,40-42]. The recent innovation of neutrino oscillations seems to give credence to the postulates of Mr. Mahendra Kumar Trivedi on the Trivedi Effect<sup>®</sup> [15]. Thus, it can be assumed that the Trivedi Effect<sup>®</sup>-Consciousness Energy Healing Treatment might be providing the necessary energy for the neutrino oscillations leads to the modification of the fundamental physicochemical properties of a compound [43,44]. The increased isotopic abundance ratios  $^2\text{H}/^1\text{H}$  or  $^{13}\text{C}/^{12}\text{C}$  or  $^{17}\text{O}/^{16}\text{O}$  or  $^{18}\text{O}/^{16}\text{O}$  would highly influence the atomic bond vibration and increase bond strength of treated cholecalciferol [45]. The alteration in the isotopic abundance ratio of the atoms/molecules cause of the change in the kinetic isotope effects, which is very useful to study the reaction mechanism, understand the enzymatic transition state, and enzyme mechanism that is supportive for

designing effective, and specific inhibitors, etc. [34]. Therefore, The Biofield Energy Treated cholecalciferol with improved isotopic abundance ratio ( $P_{M+1}/P_M$  and  $P_{M+2}/P_M$ ) might be advantageous for the better nutraceutical and pharmaceutical formulations.

#### Gas chromatography-mass spectrometry (GC-MS) analysis

The GC-MS chromatograms of the control and Biofield Energy Treated cholecalciferol showed two clear independent peaks (**Figure 3**). The  $R_t$  of the control sample was at 23.28 and 23.88 min, whereas Biofield Energy Treated sample at 23.28 and 23.88 min showed that the  $R_t$  of both the sample is very close. Therefore, the results indicated that the polarity of the Biofield Energy Treated cholecalciferol remained close compared to the control sample. The chromatograms of both the control and Biofield Energy Treated showed two peaks might be due to the *cis* and *trans* isomers of cholecalciferol [46,47].

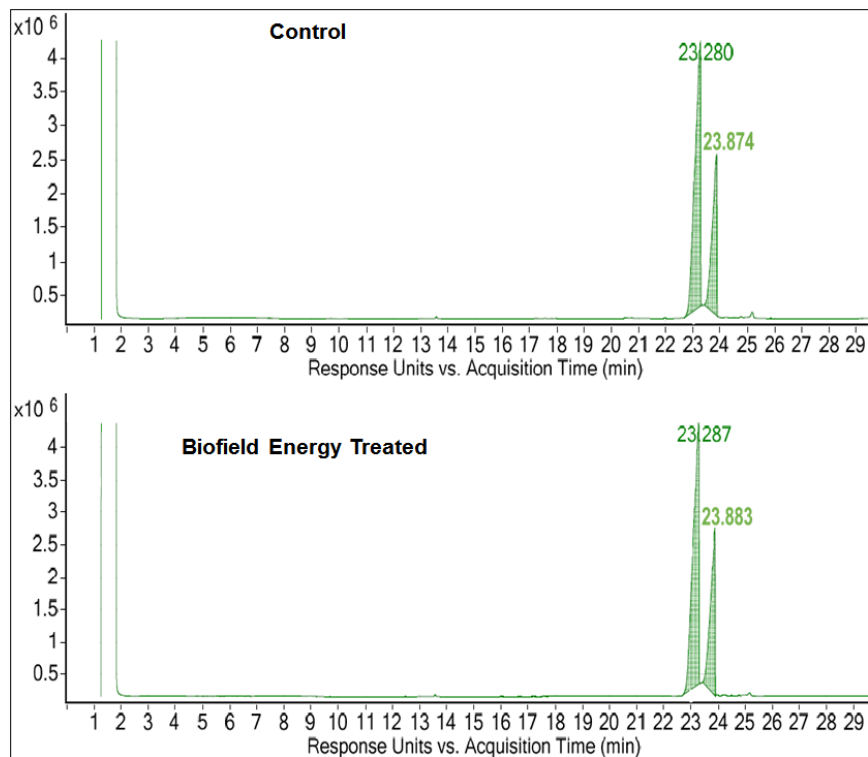


**Figure 3.** GC chromatograms of the control and treated cholecalciferol.

The GC-MS spectra of the control and treated samples at  $R_t$  of 23.28 min exhibited the presence of the molecular ion of cholecalciferol ( $C_{27}H_{44}O^+$ ) (**Figure 4**) at  $m/z$  384.4 (calcd for  $C_{27}H_{44}O^+$ , 384.34). The lower mass fragmentation peak at  $m/z$  366, 351.4 and 325.3 for  $C_{27}H_{42}^{++}$ ,  $C_{26}H_{39}^{++}$  and  $C_{24}H_{37}^+$ , respectively in both the spectra (**Figure 4**). The mass fragmentation pattern of the Biofield Energy Treated cholecalciferol was similar to that of the control sample. But the mass peak intensities of the treated cholecalciferol were altered compared to the control sample. The mass peak intensity of the control and treated cholecalciferol were 1384814.88 and 1447749.88, respectively at  $R_t$  of 23.28 min. Similarly, the mass peak intensities of the control and

Biofield Energy Treated cholecalciferol were 1219705.00 and 1258803.38, respectively at  $R_t$  of 23.88 min. The mass peak intensities at  $R_t$  23.28 and 23.88 min in the Biofield Energy Treated sample were increased by 4.54% and 3.21%, respectively compared to the control sample (**Table 2**). The mass peak intensities were significantly increased which might be possible due to the impact of the Trivedi Effect<sup>®</sup>-Consciousness Energy Healing Treatment. The Trivedi Effect<sup>®</sup> is a proved natural phenomenon which has the remarkable potential to alter the isotopic abundance ratios of various compounds through the possible mediation of neutrinos [15,43,44].

**Table 2.** GC-MS chromatographic and mass spectra analysis at  $R_t$  23.28 and 23.88 min of the control and treated cholecalciferol.

Parameters	Control sample	Biofield Energy Treated sample	% Change
Mass peak ( $m/z=384$ ) intensity at $R_t$ 23.28 min	1384814.88	1447749.88	4.54
Mass peak ( $m/z=384$ ) intensity at $R_t$ 23.88 min	1219705.00	1258803.38	3.21

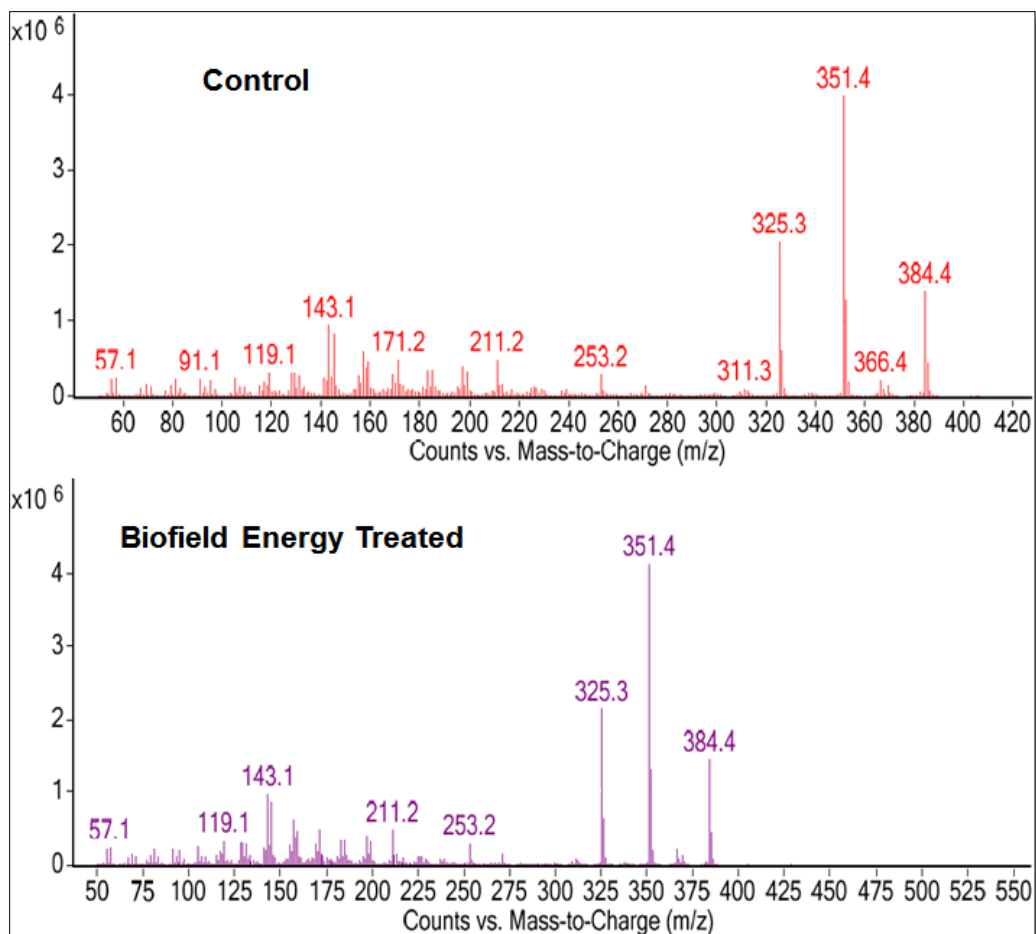


**Figure 4.** GC-MS spectra of the control and treated cholecalciferol at  $R_t$  23.28 min.

#### Nuclear magnetic resonance (NMR) spectroscopy analysis

Figures 5 and 6 showed the  $^1\text{H}$ , and  $^{13}\text{C}$  NMR spectra, respectively for the control and Biofield Energy Treated cholecalciferol. The analyzed NMR spectral data of both the samples are presented in Table 3. The  $^1\text{H}$  NMR spectra of both the samples indicated that signals for the protons coupling of  $\text{CH}_3$ ,  $\text{CH}_2$ ,  $\text{CH}$  and  $\text{OH}$  protons of cholecalciferol were in the range of  $\delta$  0.48 to 6.19 ppm (Figure 5 and Table 3), which were very close to each

other. Similarly, the carbon signals for  $\text{CH}_3$ ,  $\text{CH}_2$ ,  $\text{CH}$ ,  $=\text{C}$  and  $\text{C-OH}$  groups in the  $^{13}\text{C}$  NMR spectrum (Figure 6) were in the range of 11.74-145.45 in both the control and Biofield Energy Treated samples of cholecalciferol (Table 3). The experimental results were closely matched to the reported literature [48]. The  $^1\text{H}$  and  $^{13}\text{C}$  NMR spectral data concluded that there was no structural modification of the treated cholecalciferol compared to the control sample.

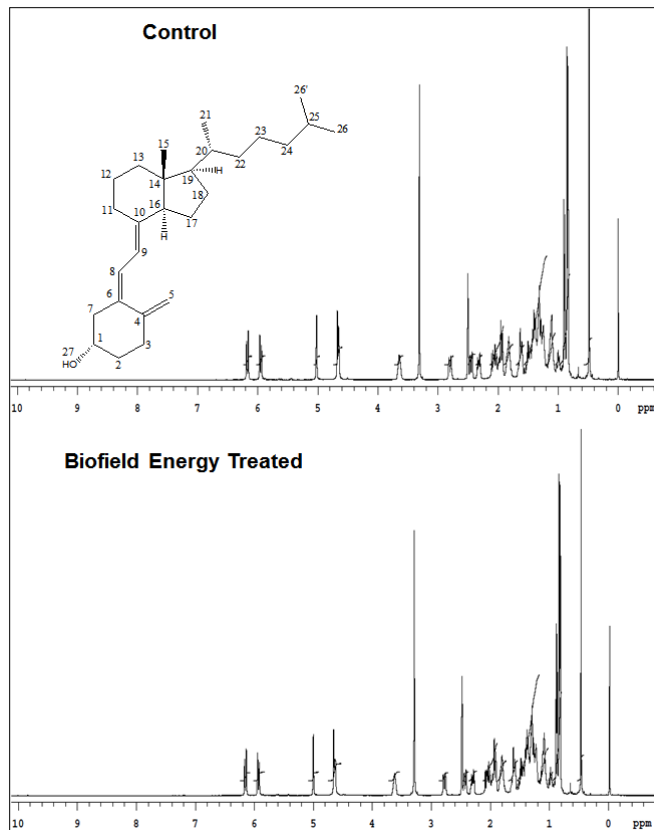


Figure 5. <sup>1</sup>H NMR spectra of the control and treated cholecalciferol.

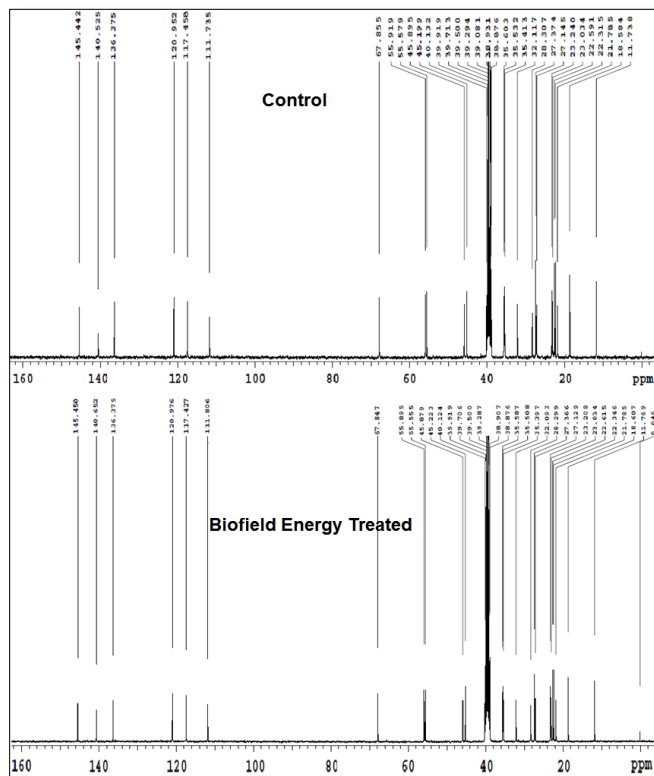


Figure 6. <sup>13</sup>C NMR spectra of the control and treated cholecalciferol.



**Table 3.**  $^1\text{H}$  and  $^{13}\text{C}$  NMR spectroscopic data of both the control and treated cholecalciferol.

$^1\text{H}$ & $^{13}\text{C}$ S. No	$^1\text{H}$ NMR $\delta$ (ppm) and Multiplicity		$^{13}\text{C}$ NMR $\delta$ (ppm)	
	Control	Biofield Energy Treated	Control	Biofield Energy Treated
1	3.65 (m, $J=20$ Hz, H)	3.65 (m, $J=20$ Hz, H)	67.86	67.85
2	1.65 (m, $J=24$ Hz, 2H)	1.65 (m, $J=24$ Hz, 2H)	35.41	35.40
3	1.81 (m, $J=24$ Hz, 2H)	1.81 (m, $J=24$ Hz, 2H)	32.12	32.10
4	--	--	136.38	136.38
5	4.67 (d, $J=12$ Hz, 2H)	d (4.66, $J=12$ Hz, 2H)	111.74	111.81
6	--	--	145.44	145.45
7	1.93-2.11 (m, 2H)	1.93-2.11 (m, 2H)	45.90	45.88
8	6.17 (d, $J=12$ Hz, H)	6.17 (d, $J=12$ Hz, 2H)	120.95	120.98
9	5.95 (d, $J=12$ Hz, H)	5.95 (d, $J=12$ Hz, H)	117.46	117.43
10	--	--	140.53	140.65
11	1.93-2.11 (m, 2H)	1.93-2.11 (m, 2H)	28.31	28.30
12	0.96-1.20 (m, 2H)	0.96-1.20 (m, 2H)	22.31	22.33
13	0.96-1.20 (m, 2H)	0.96-1.20 (m, 2H)	40.13	40.12
14	--	--	45.20	45.22
15	0.48 (S, 3H)	S(0.48, 3H)	11.74	11.77
16	2.78-2.82 (d, $J=16$ Hz, H)	2.78-2.82 (d, $J=16$ Hz, H)	55.92	55.90
17, 18, 22, 23, 24	1.25-1.43 (m, 10H)	1.25-1.43 (m, 10H)	23.03, 27.37, 35.60, 23.24, 39.92	23.03, 27.37, 35.59, 23.21, 39.92
19, 20, 25	2.11-2.50 (m, 3H)	2.11-2.47 (m, 3H)	55.60, 35.53, 27.15	55.91, 35.51, 27.13
21	0.89 (d, $J=8$ Hz, 3H)	0.89 (d, $J=8$ Hz, 3H)	18.58	18.61
26, 26'	0.86 (m, $J=12$ Hz, 6H)	m (0.86, $J=12$ Hz, 6H)	22.59, 21.79	22.61, 21.79
27(OH)	s(5.02)	s(5.02)	--	--

s: singlet; d: doublet; m: multiplet

## CONCLUSION

The present experimental data suggest that the Trivedi Effect<sup>®</sup>-Energy of Consciousness Healing Treatment has shown a significant impact on the isotopic abundance ratios and relative peak intensities of cholecalciferol/vitamin D<sub>3</sub>. The LC-MS chromatograms of both the cholecalciferol samples showed a single largest peak at the retention time ( $R_t$ ) 20.6 min and protonated molecular mass peak at  $m/z$  385.3 (calcd for  $\text{C}_{27}\text{H}_{45}\text{O}^+$ , 385.35) in the mass spectra. The LC-MS based isotopic abundance ratios of  $P_{M+1}/P_M$  ( $^2\text{H}/^1\text{H}$  or  $^{13}\text{C}/^{12}\text{C}$  or  $^{17}\text{O}/^{16}\text{O}$ ) and  $P_{M+2}/P_M$  ( $^{18}\text{O}/^{16}\text{O}$ ) were

significantly increased by 15.20% and 10.44%, respectively in the Consciousness Energy Healing Treated cholecalciferol compared to the control sample. Thus, the  $^{13}\text{C}$ ,  $^2\text{H}$ , and  $^{17}\text{O}$  contributions from  $\text{C}_{27}\text{H}_{45}\text{O}^+$  to  $m/z$  386 and  $^{18}\text{O}$  contribution from  $\text{C}_{21}\text{H}_{21}\text{O}_6^+$  to  $m/z$  387 in the Consciousness Energy Healing Treated cholecalciferol were significantly increased compared with the control sample. The GC-MS spectral data showed that the molecular mass peak intensities ( $m/z$  384.4) in the Consciousness Energy Healing Treated cholecalciferol at  $R_t$  23.28 and 23.88 min were increased by 4.54% and 3.21%, respectively compared with the control sample. The improvement in the

isotopic abundance ratios and mass peak intensities of the Consciousness Energy Healing Treated cholecalciferol might be due to the possible mediation of neutrinos *via* the Trivedi Effect<sup>®</sup>-Consciousness Energy Healing Treatment. The increased isotopic abundance ratio of the Consciousness Energy Healing Treated cholecalciferol might have a stronger atomic bond, increase the stability, and alter the rate of metabolic reactions in the body. Thus, the Trivedi Effect<sup>®</sup>-Consciousness Energy Healing Treated vitamin D<sub>3</sub> would be more advantageous to develop more efficacious nutraceutical/pharmaceutical formulations which might provide better therapeutic response against vitamin D deficiency, rickets, osteoporosis, arthritis, diabetes mellitus, multiple sclerosis, cancer, cardiovascular diseases, inflammations, infections, mental disorders, stress, aging, glucose intolerance, Parkinson's and Alzheimer's diseases, dementia, cognitive impairment in older adults, etc.

#### ACKNOWLEDGEMENT

The authors are grateful to GVK Biosciences Pvt. Ltd., Trivedi Science, Trivedi Global, Inc., Trivedi Testimonials and Trivedi Master Wellness for their assistance and support during this work.

#### REFERENCES

1. Coulston AM, Carol B, Mario F (2013) Nutrition in the prevention and treatment of disease. Academic Press 818.
2. WHO Model Formulary (2008) World Health Organization. 2009: 496.
3. Samuel S, Sitrin MD (2008) Vitamin D's role in cell proliferation and differentiation. *Nutr Rev* 66: 116-124.
4. Simana E, Simian R, Portnoy S, Jaffe A, Dekel BZ (2015) Feasibility study - Vitamin D loading determination by FTIR-ATR. *Inform Control Syst* 76: 107-111.
5. Ritu G, Gupta A (2014) Vitamin D deficiency in India: Prevalence, causalities and interventions. *Nutrients* 6: 729-775.
6. Lawson DE, Wilson PW, Kodicek E (1969) Metabolism of vitamin D. A new cholecalciferol metabolite, involving loss of hydrogen at C-1, in chick intestinal nuclei. *Biochem J* 115: 269-277.
7. Ross CA, Taylor CL, Yaktine AL, Valle HBD (2010) Dietary reference intakes for calcium and Vitamin D. Washington (DC): National Academies Press (US).
8. [https://en.wikipedia.org/wiki/Vitamin\\_D](https://en.wikipedia.org/wiki/Vitamin_D)
9. Koshy KT, Beyer WF (1984) Vitamin D<sub>3</sub> (cholecalciferol) in analytical profiles of drug substances. Florey K (Ed.) Academic Press, Inc., Orlando, USA 13: 656-707.
10. Collins ED, Norman AW (2001) Vitamin D in Handbook of Vitamins 3rd Edn. Rucker RB, Suttie JW, McCormick DB, Machlin LJ, Marcel Dekker, Inc., New York, pp: 51-114.
11. Lehmann U, Hirche F, Stangl GI, Hinz K, Westphal S, et al. (2013) Bioavailability of vitamin D(2) and D(3) in healthy volunteers, a randomized placebo-controlled trial. *J Clin Endocrinol Metab* 98: 4339-4345.
12. Branton A, Jana S (2017) Effect of the biofield energy healing treatment on the pharmacokinetics of 25-hydroxyvitamin D<sub>3</sub> [25(OH)D<sub>3</sub>] in rats after a single oral dose of vitamin D<sub>3</sub>. *Am J Pharmacol Phytother* 2: 11-18.
13. Branton A, Jana S (2017) The influence of energy of consciousness healing treatment on low bioavailable resveratrol in male Sprague Dawley rats. *Int J Clin Dev Anatomy* 3: 9-15.
14. Branton A, Jana S (2017) The use of novel and unique biofield energy healing treatment for the improvement of poorly bioavailable compound, berberine in male Sprague Dawley rats. *Am J Clin Exp Med* 5: 138-144.
15. Trivedi MK, Mohan TRR (2016) Biofield energy signals, energy transmission and neutrinos. *Am J Modern Phys* 5: 172-176.
16. Rubik B, Muehsam D, Hammerschlag R, Jain S (2015) Biofield science and healing: History, terminology and concepts. *Glob Adv Health Med* 4: 8-14.
17. Warber SL, Cornelio D, Straughn, J, Kile G (2004) Biofield energy healing from the inside. *J Altern Complement Med* 10: 1107-1113.
18. Movaffaghi Z, Farsi M (2009) Biofield therapies: Biophysical basis and biological regulations? *Complement Ther Clin Pr* 15: 35-37.
19. Koithan M (2009) Introducing complementary and alternative therapies. *J Nurse Pract* 5: 18-20.
20. Trivedi MK, Nayak G, Patil S, Tallapragada RM, Latiyal O (2015) Impact of biofield treatment on physical, structural and spectral properties of antimony sulfide. *Ind Eng Manage* 4:165.
21. Trivedi MK, Nayak G, Patil S, Tallapragada RM, Latiyal O (2015) Studies of the atomic and crystalline characteristics of ceramic oxide nano powders after bio field treatment. *Ind Eng Manage* 4: 161.
22. Trivedi MK, Branton A, Trivedi D, Nayak G, Singh R, et al. (2015) Characterization of physical, thermal and spectroscopic properties of biofield energy treated p-phenylenediamine and p-toluidine. *J Environ Anal Toxicol* 5: 329.

23. Trivedi MK, Branton A, Trivedi D, Nayak G, Singh R, et al. (2015) Characterization of biofield energy treated 3-chloronitrobenzene: Physical, thermal and spectroscopic studies. *J Waste Resour* 5:183.
24. Trivedi MK, Branton A, Trivedi D, Nayak G, Balmer AJ, et al. (2017) Evaluation of physicochemical, thermal, structural, and behavioral properties of magnesium gluconate treated with energy of consciousness (the Trivedi Effect®). *J Drug Design Med Chem* 3: 5-17.
25. Trivedi MK, Branton A, Trivedi D, Nayak G, Bairwa K, et al. (2015) Spectroscopic characterization of disulfiram and nicotinic acid after biofield treatment. *J Anal Bioanal Tech* 6: 265.
26. Trivedi MK, Patil S, Shettigar H, Singh R, Jana S (2015) An impact of biofield treatment on spectroscopic characterization of pharmaceutical compounds. *Mod Chem Appl* 3: 159.
27. Trivedi MK, Branton A, Trivedi D, Nayak G, Bairwa K, et al. (2015) Effect of biofield treatment on physical, thermal, and spectral properties of SFRE 199-1 mammalian cell culture medium. *Adv Biochem* 3: 77-85.
28. Trivedi MK, Branton A, Trivedi D, Nayak G, Bairwa K, et al. (2015) Physicochemical and spectroscopic properties of biofield energy treated protose. *Am J Biomed Life Sci* 3: 104-110.
29. Trivedi MK, Branton A, Trivedi D, Nayak G, Gangwar M, et al. (2015) Agronomic characteristics, growth analysis, and yield response of biofield treated mustard, cowpea, horse gram and groundnuts. *Int J Genet Genomics* 3: 74-80.
30. Trivedi MK, Branton A, Trivedi D, Nayak G, Saikia G, et al. (2015) Quantitative determination of isotopic abundance ratio of  $^{13}\text{C}$ ,  $^2\text{H}$  and  $^{18}\text{O}$  in biofield energy treated ortho and meta toluic acid isomers. *Am J Appl Chem* 3: 217-223.
31. Trivedi MK, Branton A, Trivedi D, Nayak G, Panda P, et al. (2016) Evaluation of the isotopic abundance ratio in biofield energy treated resorcinol using gas chromatography-mass spectrometry technique. *Pharm Anal Acta* 7: 481.
32. Trivedi MK, Branton A, Trivedi D, Nayak G, Panda P, et al. (2016) Gas chromatography-mass spectrometric analysis of isotopic abundance of  $^{13}\text{C}$ ,  $^2\text{H}$  and  $^{18}\text{O}$  in biofield energy treated p-tertiary butylphenol (PTBP). *Am J Chem Eng* 4: 78-86.
33. Schellekens RC, Stellaard F, Woerdenbag HJ, Frijlink HW, Kosterink JG (2011) Applications of stable isotopes in clinical pharmacology. *Br J Clin Pharmacol* 72: 879-897.
34. Muccio Z, Jackson GP (2009) Isotope ratio mass spectrometry. *Analyst* 134: 213-222.
35. Weisel CP, Park S, Pyo H, Mohan K, Witz G (2003) Use of stable isotopically labeled benzene to evaluate environmental exposures. *J Expo Anal Environ Epidemiol* 13: 393-402.
36. Rosman KJR, Taylor PDP (1998) Isotopic compositions of the elements 1997 (Technical Report). *Pure Appl Chem* 70: 217-235.
37. Smith RM (2004) Understanding mass spectra: A basic approach. 2nd Edn. John Wiley & Sons Inc., ISBN 0-471-42949-X.
38. Jürgen H (2004) Gross mass spectrometry: A textbook. 2nd Edn. Springer: Berlin.
39. Meija J, Coplen TB, Berglund M, Brand WA, De Bièvre P, et al. (2016) Isotopic compositions of the elements 2013 (IUPAC technical report). *Pure Appl Chem* 88: 293-306.
40. Kajita T (2010) Atmospheric neutrinos and discovery of neutrino oscillations. *Proc Jpn Acad Series B Phys Biol Sci* 86: 303-321.
41. McDonald AB (2015) The Sudbury neutrino observatory: Observation of flavor change for solar neutrinos: Lecture slides Nobel Lecture, Aula Magna, Stockholm University.
42. Kajita T (2015) Discovery of atmospheric neutrino oscillations: Lecture slides, Nobel lecture, Aula Magna, Stockholm University.
43. Trivedi MK, Branton A, Trivedi D, Nayak G, Panda P, et al. (2016) Gas chromatography-mass spectrometric analysis of isotopic abundance of  $^{13}\text{C}$ ,  $^2\text{H}$  and  $^{18}\text{O}$  in biofield energy treated p-tertiary butylphenol (PTBP). *Am J Chem Eng* 4: 78-86.
44. Trivedi MK, Branton A, Trivedi D, Nayak G, Panda P, et al. (2016) Evaluation of the isotopic abundance ratio in biofield energy treated resorcinol using gas chromatography-mass spectrometry technique. *Pharm Anal Acta* 7: 481.
45. Santesteban LG, Miranda C, Barbarin I, Royo JB (2014) Application of the measurement of the natural abundance of stable isotopes in viticulture: A review. *Austr J Grape Wine Res* 21: 157-167.
46. Holick MF, Garabedian M, DeLuca HF (1972) 5,6-Trans isomers of cholecalciferol and 25-hydroxycholecalciferol. Substitutes for 1,25-dihydroxycholecalciferol in anephric animals. *Biochemistry* 11: 2715-2719.
47. Okamura WH, Midland MM, Hammond MW, Abd Rahman N, Dormanen MC, et al. (1995) Chemistry and

conformation of vitamin D molecules. *J Steroid Biochem Mol Biol* 53: 603-613.

48. Florey K (1984) *Analytical profiles of drug substances*. Academic Press Inc. 13: 665-715.